



Counterflow flames of ultrahigh-molecular-weight polyethylene with and without triphenylphosphate



O.P. Korobeinichev^{a,*}, M.B. Gonchikzhapov^{a,b}, A.A. Paletsky^a, A.G. Tereshchenko^a,
I.K. Shundrina^{b,c}, L.V. Kuibida^{a,b}, A.G. Shmakov^{a,b}, Y. Hu^d

^a Voevodsky Institute of Chemical Kinetics and Combustion, Institutskaya str. 3, Novosibirsk 630090, Russia

^b Novosibirsk State University, Pirogova str. 2, Novosibirsk 630090, Russia

^c Novosibirsk Institute of Organic Chemistry, Lavrentiev Avenue 9, Novosibirsk 630090, Russia

^d State Key Laboratory of Fire Science, University of Science and Technology of China, Hefei 230027, China

ARTICLE INFO

Article history:

Received 2 September 2015

Revised 20 April 2016

Accepted 21 April 2016

Available online 17 May 2016

Keywords:

Counterflow flame of polymer

Flame retardancy

Flame structure

Polymer flammability

Phosphorus-containing compounds

Thermal degradation of polymers

ABSTRACT

To study the mechanism of flame retardancy, counter-flow flames of air and ultrahigh-molecular-weight polyethylene (UHMWPE) with triphenylphosphate (TPP) added, and also without it, were studied at atmospheric pressure. Burning rates were measured. Also the thermal and chemical structure of these counter-flow flames (with and without TPP added) was investigated. The concentrations of the heavy products from the polymer's thermal degradation were measured by sampling the flame at 0.8 mm from the polymer's surface. Temperature profiles in both the flame and the condensed phase were measured, as well as the temperature of the polymer's burning surface, the concentration profiles of 8 species (N_2 , O_2 , CO_2 , CO , H_2O , C_3H_6 , C_4H_6 , C_6H_6) and finally the concentration profile for a hypothetical species, whose molecular weight was the average of more than 50 hydrocarbons containing C_7 – C_{25} . The effect of adding TPP to UHMWPE on all the above characteristics indicates that TPP changes what is occurring in both the condensed phase and in the flame. Chromatography and FTIR spectroscopy revealed the formation of phosphorus-containing compounds (phosphates, ethers, and carbonates) on the surface of the burning polymer. Elemental analysis showed half the TPP additive remains in the condensed phase and half goes into the flame. Adding 5 wt% of TPP to UHMWPE reduced the burning rate; also the composition of the heavy products from the destruction of this polyethylene was changed markedly by the additive. In fact, the maximum in the distribution of heavy hydrocarbons shifted towards lighter masses. All these facts indicate that TPP does have a real effect in the condensed phase. However, the lowering of the polymer's flammability was ascribed to the effect of TPP on gas-phase processes, as manifested by: a widening of the flame front, a decrease in the maximum flame temperature and a reduction of the extinction strain rate. Overall, these observations do indicate that TPP (a retardant of hydrocarbon flames) reduces the flammability of UHMWPE by a gas-phase mechanism.

© 2016 The Combustion Institute. Published by Elsevier Inc. All rights reserved.

1. Introduction

The wide use of polymeric materials requires a high level of fire safety. Polyethylene is one of the most widely used polymers. Ultrahigh-molecular-weight polyethylene is a prospective structural material, because of its unique physical and mechanical properties, particularly under extreme conditions [1]. One of the key issues regarding the mechanism of flame retardancy is the problem of where a retardant acts – is it in the condensed phase or the gas phase? A flame retardant may alter the thermal degradation of

the polymer, as well as the oxidizing reactions of the combustible products from the polymer's thermal degradation in the flame. Studying a counterflow flame of a polymer burning in air is one effective method of studying the mechanism of a polymer's combustion [2–7]. Previously [2] counterflow flames of different polymers have been studied, including those of high molecular weight ($MW \sim 8 \times 10^5$ to 8×10^6) polyethylene; also the dependence of the burning rates of certain polymers on the oxidizer's flow velocity was measured. It was shown that the stagnation plane of the flows of oxidizer and fuel was between the polymer's surface and the flame front. Temperature profiles in the gas and condensed phases were measured for non-charring and charring materials. The structure of a counterflow flame of low density polyethylene (LDPE, $MW \sim 5 \times 10^5$) was studied [3] at atmospheric pressure using a quartz

* Corresponding author. Fax: +7 383 330 73 50.

E-mail address: korobein@kinetics.nsc.ru, okorobeinichev@gmail.com (O.P. Korobeinichev).

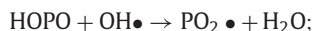
microprobe to sample the hot gas. In addition, temperature profiles were measured with a thermocouple. The oxygen concentration was 21.2, 23.2 or 25.3 vol%. Concentrations of H₂ and H₂O were calculated using material balances. Profiles of the total concentrations: {[CO]+[CH₄]}, as well as {[C₂H₂]+[C₂H₄]}, were measured [3]. The mass burning rate for [O₂]=25.3 vol% was 6.6 g/m² s; the linear burning rate was 7.3 × 10⁻³ mm/s; the temperature of the burning surface was 630 °C; the width of the zone where oxygen was consumed was ~4 mm. The mole fraction of oxygen near the burning surface was evaluated [3] to be ~5.4 × 10⁻³, using the estimated concentration gradient of oxygen near the burning surface. It was assumed that monomers were formed during the pyrolysis of polyethylene. Also, it did prove possible to estimate an upper limit for the rate of diffusion of oxygen to the fuel's surface. The enthalpy released by oxidizing the polymer pyrolysed 20% of the fuel.

The pyrolysis of LDPE and high-density polyethylene (HDPE, MW ~ 3 × 10⁵), as well as of low-density polyethylene (LDPE, MW ~ 5 × 10⁵) has been studied [5] by thermal analysis. Also, the structure of a counterflow flame of polymer was investigated similarly to [2]. Saturated hydrocarbons and hydrocarbons with one olefinic bond were found to be the main gaseous products of LDPE being pyrolysed at 700 °C. To study the kinetics of HDPE pyrolysis in hot air diluted with water vapor or carbon dioxide, the counterflow flame of HDPE/air diluted with water vapor or carbon dioxide was investigated [6]. The kinetic parameters obtained with this method were different from those obtained using a TGA. The structure of the counterflow flame of polymethylmethacrylate (PMMA) has been studied [7], as also has the composition of the pyrolysis products of LDPE (MW = 15,000) [8]. In addition, the effect of the high heating rate on the concentrations of the products from the thermal degradation of HDPE (MW = 1000) has been investigated [9]. The influence of triphenylphosphate (TPP) additive as a flame retardant on both the combustion and thermal degradation of polymers has studied [10–14]. Thus, it was shown [10] using FTIR spectroscopy and chromatography, that TPP influences the composition of the products in the condensed phase from degrading polycarbonate (PC). It was supposed [10] that the formation of phosphates stabilizes PC during its degradation by forming branched phosphorus structures. These structures play the role of a heat barrier and so reduce the flow of the combustible products from the PC surface during its burning. Phosphates were found both in the products formed by degrading PC and in the resulting char. However, the authors [10] believe that phosphates are more effective in the gas phase.

The pyrolysis of PC and PC/acrylonitrile–butadiene–styrene (ABC) with and without TPP was investigated by thermal analysis [11–13]. Phosphorus-based mechanisms of flame retardancy have been discussed [13]. A study [14] of the enhancement of a polystyrene's degradation with a flame retardant added revealed that sulphur additives and TPP exert a synergistic action, when reducing a polystyrene's flammability.

The impact of TPP on thermal degradation and the candle-like burning of UHMWPE was investigated [15–16] with molecular-beam mass spectrometry, as well as with microthermocouples, chromatography and the standard methods of testing a material's flammability. Adding TPP to UHMWPE inhibited its thermal degradation in an inert atmosphere only at high heating rates (~150 K/s) and did not influence it at low heating rates (0.17 K/s). The burning rate of UHMWPE approximately halved, when 5 wt% of TPP was added; also the flame temperature went down by 400 °C at a distance of 5 mm from the burning surface [15]. The temperature of the burning surface of UHMWPE was 670 °C. The main combustion products were propylene (27 wt%), butadiene (43 wt%), and benzene (8 wt%). In these experiments, a sonic probe and a molecular beam inlet system were used for on-line sampling of flame

gases into a time-of-flight mass spectrometer (TOFMS). TPP vapors were found in the flame during candle-like burning of UHMWPE with TPP added. The chemistry of the combustion of organophosphorus compounds (OPC), as well as the mechanisms of their impact on the flame propagation velocity, the flame structure, and the flame propagation limits of hydrogen and hydrocarbon flames, have been discussed [17]. Flame inhibition with OPC additives was shown [17] to occur by accelerating the recombination rate of H and OH radicals in their reactions with oxides and oxyacids of phosphorus:



Adding flame retardants, like hexabromocyclododecane, triphenylphosphine oxide, TPP, and sulphur, to a premixed methane-air flame resulted in a reduction of the concentrations of H and OH radicals [14,18–20]. TPP (0.019 wt%) seems to be the most effective flame retardant, roughly halving the radicals' concentrations.

Thus, there is information in the literature on the burning rates and structures of counterflow flames of polyethylene with different molecular weights. Ethylene and hydrocarbons with low molecular weight are the main products of thermal degradation. However, a large fraction of heavy hydrocarbons in the products from degrading polyethylene was also found [9]. Analysis of the literature has shown that the composition of the products of thermal degradation strongly depends on the experimental conditions and on the polyethylene (LDPE, HDPE or UHMWPE). The flame structure was elucidated by supposing that the thermal degradation of polyethylene yields only monomers and no products. The gas phase mechanism of flame inhibition with OPC additives is described in the literature quite well [17]. However, there are no publications on the effects of flame retardant additives, including OPC, on counterflow flames of polymers.

Some researchers [11–13] believe a flame retardant acts in the gas phase, if thermal analysis shows that the additive does not influence the thermal degradation of the polymer. However, thermal analysis is usually used under conditions of low heating rates (0.17 K/s) and at temperatures lower than those observed at ignition and combustion. As mentioned above [15,16], it is only at a high heating rate (150 K/s) and high temperatures close to those at ignition and combustion of the polymer, that a flame retardant inhibits the decomposition of UHMWPE. Thus, the above supposition, based on thermal analysis, is not always applicable. Therefore, a counterflow flame was used in this study. Its objective was to investigate a counterflow diffusion flame of UHMWPE with and without TPP added, in order to improve our understanding of how TPP retards a flame of UHMWPE.

2. Experimental

2.1. Materials

The specimens were pressed from UHMWPE powder with a grain size ~60 μm (MW ~2.5 × 10⁶, *T*_{melt} = 142 °C) synthesized in the Institute of Catalysis (S.B., Russian Academy of Sciences), together with its mixture with TPP (crystal size ~40 to 60 μm, MW ~326, *T*_{melt} = 40–50 °C, Aldrich, CAS number: 115-86-6). Mixtures of UHMWPE + TPP 95/5 (wt%) powders were used in the study and were prepared by mechanical mixing for 15–20 min. Specimens of UHMWPE and UHMWPE + TPP (14 mm diam. and 30–40 mm long) were prepared by hot pressing powders at 140 °C and a pressure of 100 atm. The density of the UHMWPE was 0.92 g/cm³; when 5 wt% TPP was added, the density changed insignificantly to 0.94 g/cm³.

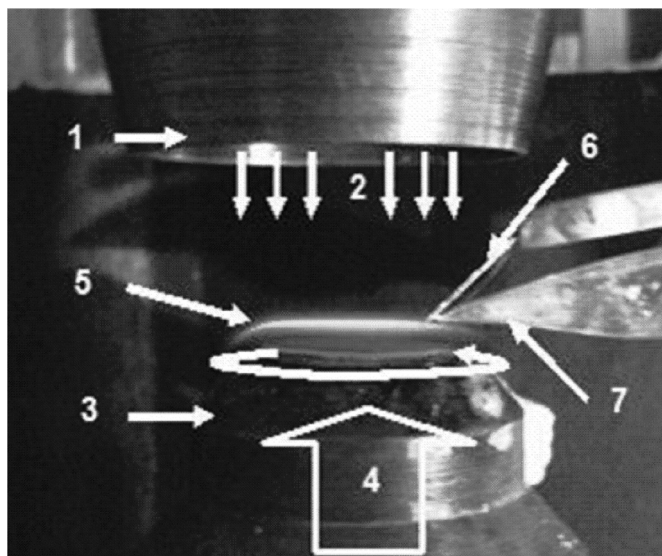


Fig. 1. A photograph of the burner: 1 – nozzle, 2 – air flow, 3 – thermostated jacket, 4 – a polymer sample inside the jacket, 5 – flame, 6 – thermocouple, 7 – quartz probe.

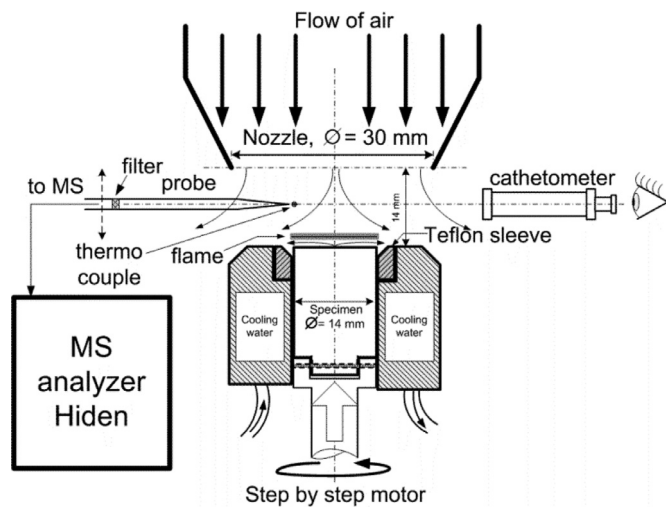


Fig. 2. A schematic diagram of the experimental set-up.

2.2. Experimental setup

The structure of a counterflow flame of polymer was investigated using a specially designed burner, similar to those used [2–5] previously. The burner incorporated a mechanism for moving the specimen and a nozzle of a special shape, with which the flow of air was directed at the polymer's surface. A photograph of the burner and a schematic diagram of the setup are shown in Figs. 1 and 2. For this burner, two stepper motors were used, one of which served to rotate the specimen around its axis; the second one moved the specimen along the axis. The specimens were rotated with a frequency of ~ 1 Hz inside a thermostated (70°C) metal jacket. Rotation was required for uniform heating of the specimen, which was ignited with a glowing nichrome spiral. After removing the igniter, the specimen burned in self-sustained conditions. The upper part of the specimen (~ 4 mm) was insulated from the walls of the metal jacket with a teflon ring, which prevented cooling of the upper melted layer of UHMWPE during burning. The distance between the nozzle and the polymer's surface was 14 mm. The air velocity (under normal conditions) at the exit from the nozzle was

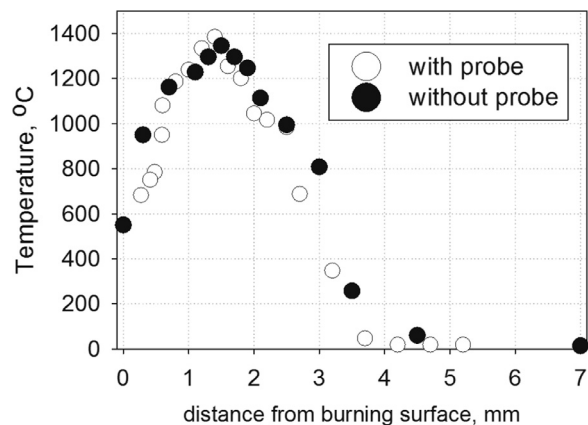


Fig. 3. The temperature profiles in a flame of UHMWPE with and without a probe.

43.9 cm/s and was set with an MKS flow controller (Type 247, dev. 0.3%). The accuracy of measuring the air velocity was ± 0.13 cm/s. A flame was stabilized by moving the specimen with the second stepper motor at a fixed velocity equal to the burning rate. The accuracy of stabilizing the surface of the burning sample was less than 5×10^{-2} mm after being controlled with a cathetometer. The flame gases were sampled with a quartz probe with an orifice diameter of 6×10^{-2} mm, wall thickness of 0.14 mm and an internal angle of 20° . The minimum possible distance between the tip of the probe and the burning surface was 0.7 mm. The probe was positioned in relation to the burning surface during an experiment with a 3D-coordinate device and a cathetometer with an accuracy of $\pm 10^{-2}$ mm. In order to minimize perturbations of a flame by the probe, flame gases were sampled at a distance of ~ 5 mm from the specimen's axis. The volumetric flow rate of gas through the probe was $0.5 \text{ cm}^3/\text{s}$ and $0.24 \text{ cm}^3/\text{s}$ under normal conditions at temperatures of 300 K and 1400 K, respectively. The composition of the gas sample was analyzed on-line with a mass spectrometric complex (Hiden HPR 60), based on a quadrupole mass spectrometer. The sample was delivered from the flame to the mass spectrometer's inlet system, where the pressure was 5×10^{-3} Torr, using a teflon tube (1.5 m long, i.d. 4 mm) with two fine filters. The energy of the ionizing electrons in the ion source was 70 eV.

The flame temperature was measured with a Pt–Pt/Rh (10%) thermocouple of $50 \mu\text{m}$ diameter, coated with a thin layer of SiO_2 ($10 \mu\text{m}$) to prevent catalytic processes; the thermocouple had shoulders of 8 mm diameter. To take the probe perturbations into account, the thermocouple was placed at a distance of $350 \mu\text{m}$ from the probe's tip. The measured temperature profiles in flame in the absence of the probe (Fig. 3) showed the width of the combustion zone to be equal to 4.3 mm. Considering corrections for radiation, the maximum temperature was deemed to be 1380°C , which was very close to the measurements with the probe. Thus, the probe did not perturb the thermal structure of the flame significantly. To measure the temperature in the condensed phase, the thermocouple was embedded into the specimen, as shown in Fig. 4. For this purpose, holes of 0.5 mm in diameter were drilled in the specimen at angle of 150° ; then a Pt–Pt/Rh(10%) thermocouple of diameter 5×10^{-2} mm was inserted into the channel. The channel was finally melted at the edges of the specimen to rule out any subsequent shifting of the thermocouple. A similar approach was used before [21] to measure the burning surface's temperature during the combustion of PMMA.

When measuring the temperature, a 14-bit analog-digital converter E14-140-M ("L-Card") was used. The analog-digital converter for the thermocouple's data acquisition was controlled with a personal computer, which was connected with a standard USB interface.

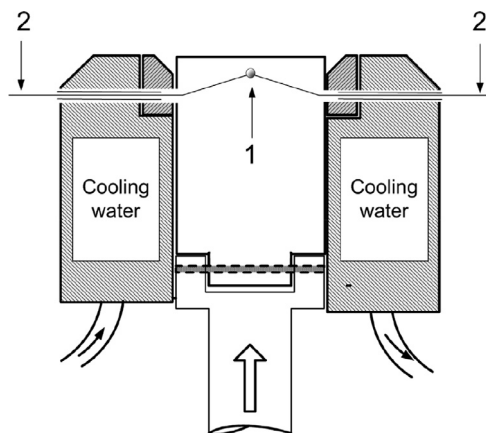


Fig. 4. Embedding a thermocouple inside the specimen. 1 – thermocouple's juncture, 2 – thermocouple leads.

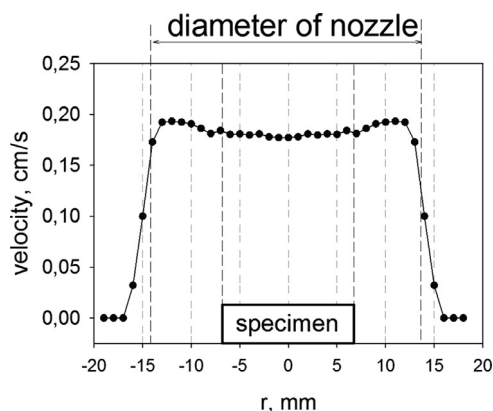


Fig. 5. The radial profile of the gas flow velocity at the distance of 5 mm from the nozzle's exit.

To provide a uniform flow of oxidizer, a converging nozzle was used. Shown in Fig. 5 is the profile of the air velocity over a cross-section at 5 mm from the nozzle's exit. It was measured with a wire anemometer, based on a platinum wire 1×10^{-2} mm in diameter. The velocity of the air was in the range of 0.1–2 m/s; it was measured to an accuracy of 1%.

2.3. Gas chromatographic/mass spectrometric analysis of samples taken from the flame and from the burning surface

To identify species in the combustion products near the burning surface of UHMWPE, a gas–liquid chromatograph coupled with a

mass spectrometer (GLC/MS) was used. With a syringe (steel capillary 0.7 mm o.d.) a sample of gas $\sim 1 \text{ cm}^3$ in volume was taken from the blue flame zone at a distance of 0.8 mm from the burning surface. A white coating of condensed pyrolysis products of UHMWPE was deposited on the walls of the syringe. The samples were analyzed with an Agilent HP 6890 N/5973 N gas chromatograph with a column of the DB-1 type. Mass spectra were interpreted automatically using standard software for a gas chromatograph plus mass spectrometer. Because the DB-1 siloxane column does not allow separation of N_2 , CO_2 and CO by retention time, additional analysis of the gas sample was made with the Kristall 2000 chromatograph with a zeolite-coal column. The flame gases were sampled using a quartz probe (diam. of orifice 6×10^{-2} mm) at 0.8 mm from the burning surface. The products formed on the UHMWPE/TPP burning surface were analyzed using a liquid LC Agilent Technologies 1200/MS microTOF-Q Bruker Daltonics chromatograph with a Precol+SB-C18 column. The samples were extracts of the products of the dripped melt. After several hours of soaking in acetone, the extract was separated from the undissolved residue and was introduced into the chromatograph.

2.4. FTIR and elemental analysis of the polymer specimens and of the dripped melt

IR spectra of specimens of the polymer and of the dripped melt were recorded with a Tensor 27 (Bruker) spectrometer. Elemental analyses (C, H, O) of the specimen's surface before and after combustion were performed using the Eurovector EA 3000 analyzer. The accuracy of these measurements by mass was C: 0.3%, H: 0.05%, O: 0.5%. The content of phosphorus (P) was determined by spectrophotometry of the blue phosphorus molybdenum complex with an accuracy by mass of $\pm 0.03\%$.

3. Results and discussion

3.1. The burning rate of UHMWPE and UHMWPE + 5 wt% of TPP

Shown in Fig. 6A is a photograph of a counter-flow flame of UHMWPE. It can be seen that the probe does not cause any substantial perturbations of the flame during sampling. The distance from the polymer's surface to the middle of the glowing zone was 1.7 mm; the width of the glowing zone was 1.3 mm; the polymer melt was dripping from the specimen's surface during combustion. Table 1 presents data relating to the burning rate of UHMWPE and UHMWPE + 5 wt% of TPP. Here M_1 is the total mass burning rate, M_2 is the mass burning rate minus the mass rate of dripping from the burning surface, u is the burning rate, as calculated by measuring the length of the burnt specimen and the time of its burning.

When TPP was added to UHMWPE, the flame's color changed to light turquoise. The width of the glowing zone increased from

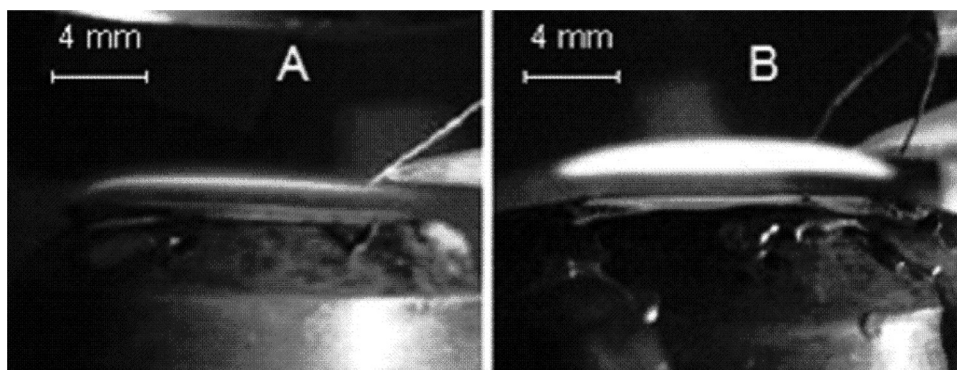


Fig. 6. Photographs of flames: A – UHMWPE, B – UHMWPE+5 wt% of TPP.

Table 1

The burning rates of UHMWPE and UHMWPE+5 wt% of TPP.

Specimen	M_1 (g/m ² s)	M_2 (g/m ² s)	u (μm/s)
UHMWPE	14.4 (±1)	9.9 (±1)	18 (±2)
UHMWPE/5 wt% of TPP	7.9 (±1)	7.2 (±1)	7.7(±1)
Ratio of burning rates without TPP and with TPP	1.83	1.4	2.3

1.3 mm to 2 mm, and the distance from the polymer's surface to the middle of the glowing zone increased from 1.7 mm to 2 mm (see Fig. 6B). Previously [15], TPP vapors were identified in the flame during candle-like burning of UHMWPE + 10 wt% of TPP. It has been shown [14] that adding TPP to a methane-air flame reduces the concentration of OH radicals by accelerating the recombination of OH radicals, thereby inhibiting the flame. This may be the cause of the flame zone widening when TPP was added to UHMWPE. When TPP was added to UHMWPE, the dripping rate decreased ~3 times; this suggests that TPP influences processes occurring in the condensed phase.

The mass burning rate of UHMWPE was higher than that measured previously [3,5]. This is likely to be related to differences in the molecular mass of the polyethylene specimens studied. When 5 wt% of TPP was added to UHMWPE, the burning rates, M_1 and u , approximately halved. A low value of the reduction in the burning rate of UHMWPE in candle-like burning, when 5 wt% of TPP was added was obtained previously [15]. The mass burning rate M_2 , related only to the products entering the gas phase, decreases much less (~1.4 times) than the burning rate u . It is also to be noted that the dripped melt changed in color from white to dark brown as 5 wt% of TPP was added to UHMWPE. The burning rates M_i and u are measured using the following formulae: $M_1 = (m_0 - m_f)/t_b S$, $M_2 = M_1 - M_3$, $u = (l_0 - l_f)/t_b$, $M_3 = m_3/t_b S$, where m_0 , m_f , m_3 , t_b , S , l_0 , l_f , M_3 are the initial mass of the specimen, its final mass after combustion, the mass of the specimen's dripping, the time of its burning, the cross section of the specimen, the initial length of the

specimen, its final length after combustion, and the mass rate of the specimen's dripping, correspondingly.

3.2. The composition of heavy hydrocarbons near the burning surface of UHMWPE and UHMWPE + 5 wt% of TPP

Table 2 shows the mass fractions of heavy hydrocarbons (C_7 – C_{25}) in the products sampled from the flame at a distance of 0.8 mm to the burning surface of UHMWPE and UHMWPE+5 wt% of TPP, obtained using GLC/MS to analyze samples of the gas and condensed phase. The data shown are averages for three experiments. Primarily, the specimens were calibrated for a mixture of alkanes (C_7 – C_{40}) after measuring their retention times and sensitivity coefficients. As a large amount of nitrogen is present in the gaseous part of the sample, the starting section of the chromatogram was blurred. Consequently we were unable to determine the percentage of propylene, butadiene, and benzene in the sample. The products contain a wide range of linear hydrocarbons from C_7 to C_{25} . Hydrocarbons with a mass greater than that of C_{25} were not found. Ethylene and methane were not found. The results were close to the composition of the degradation products obtained previously [8,9]. Figure 7 shows the distribution of heavy hydrocarbons (C_7 – C_{25}) in the products sampled from the flame at a distance of 0.8 mm from the burning surfaces of UHMWPE and UHMWPE+5 wt% of TPP, obtained on the basis of the data shown in Table 2. The mass fraction plotted in Fig. 7 for each n (the number of carbon atoms per molecule) is the sum of the mass fractions of alkane, alkene, and alkadiene for this n . The average molecular weight obtained from the product distribution (Fig. 7) was equal to 258.7 g/mol for UHMWPE and 129.7 g/mol for UHMWPE + 5 wt% of TPP.

3.3. The structure of a counterflow flame of UHMWPE without heavy hydrocarbons

According to earlier results [15], propylene (C_3H_6), butadiene (C_4H_6), and benzene (C_6H_6) are the main decomposition products

Table 2Mass fractions of heavy hydrocarbons (C_7 – C_{25}) in the products sampled at a distance of 0.8 mm from the burning surfaces of UHMWPE and UHMWPE + 5 wt% of TPP.

Species	Formula	UHMWPE (wt%)	UHMWPE + 5% TPP (wt%)	Species	Formula	UHMWPE (wt%)	UHMWPE + 5% TPP (wt%)
Heptadiene	C_7H_{12}	0	0	Hexadecane	$C_{16}H_{34}$	2.85	0.53
Heptene	C_7H_{14}	1.68	7.06	Heptadecadiene	$C_{17}H_{32}$	1.08	0.05
Heptane	C_7H_{16}	0.76	15.54	Heptadecene	$C_{17}H_{34}$	1.63	0.05
Octadiene	C_8H_{14}	0.23	2.47	Heptadecane	$C_{17}H_{36}$	0.87	0.75
Octene	C_8H_{16}	1.14	8.83	Octadecadiene	$C_{18}H_{34}$	1.67	0
Octane	C_8H_{18}	0.53	3.53	Octadecene	$C_{18}H_{36}$	8.89	1.29
Nonadiene	C_9H_{16}	0.38	3.53	Octadecane	$C_{18}H_{38}$	1.11	0.51
Nonene	C_9H_{18}	1.91	17.65	Nonadecadiene	$C_{19}H_{36}$	1.97	0
Nonane	C_9H_{20}	0.61	1.77	Nonadecene	$C_{19}H_{38}$	3.94	0.46
Decadiene	$C_{10}H_{18}$	0.37	1.02	Nonadecane	$C_{19}H_{40}$	0	0
Decene	$C_{10}H_{20}$	2.56	6.78	Eicosadiene	$C_{20}H_{38}$	1.06	0
Decane	$C_{10}H_{22}$	0.66	0.00	Eicosene	$C_{20}H_{40}$	2.11	0
Undecadiene	$C_{11}H_{20}$	0.53	0.41	Eicosane	$C_{20}H_{42}$	10.55	1.63
Undecene	$C_{11}H_{22}$	1.76	2.03	Heneicosadiene	$C_{21}H_{40}$	0.74	0
Undecane	$C_{11}H_{24}$	0.88	1.63	Heneicosene	$C_{21}H_{42}$	1.48	0
Dodecadiene	$C_{12}H_{20}$	0.42	0.00	Heneicosane	$C_{21}H_{44}$	2.95	0
Dodecene	$C_{12}H_{24}$	1.25	0.39	Docosadiene	$C_{22}H_{42}$	0.92	0
Dodecane	$C_{12}H_{26}$	0.83	9.64	Docosene	$C_{22}H_{44}$	1.83	0
Tridecadiene	$C_{13}H_{24}$	0.33	0.06	Docosane	$C_{22}H_{46}$	7.32	0.85
Tridecene	$C_{13}H_{26}$	0.99	0.06	Tricosadiene	$C_{23}H_{44}$	1.13	0
Tridecane	$C_{13}H_{28}$	0.66	0.06	Tricosene	$C_{23}H_{46}$	2.25	0
Tetradecadiene	$C_{14}H_{22}$	0.41	0.00	Tricosane	$C_{23}H_{48}$	2.25	0
Tetradecene	$C_{14}H_{28}$	1.22	0	Tetracosadiene	$C_{24}H_{46}$	0	0
Tetradecane	$C_{14}H_{30}$	0.95	0.63	Tetracosene	$C_{24}H_{48}$	2.42	0
Pentadecadiene	$C_{15}H_{28}$	0.37	0.06	Tetracosane	$C_{24}H_{50}$	6.05	0
Pentadecene	$C_{15}H_{30}$	1.48	0.06	Pentacosadiene	$C_{25}H_{48}$	2.20	0
Pentadecane	$C_{15}H_{32}$	0.92	0.06	Pentacosene	$C_{25}H_{50}$	2.20	0
Hexadecadiene	$C_{16}H_{30}$	0	0	Pentacosane	$C_{25}H_{52}$	3.30	0
Hexadecene	$C_{16}H_{32}$	1.43	0.05				

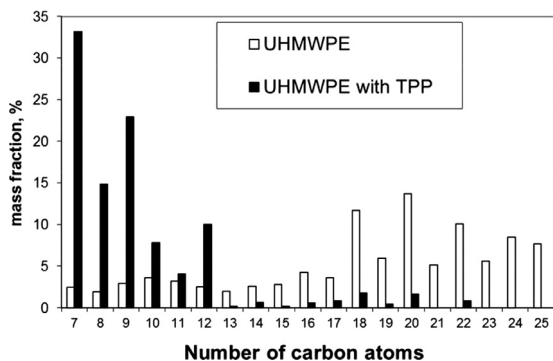


Fig. 7. Distribution of heavy hydrocarbons (C_7 – C_{25}) in the combustion products sampled from the flame at a distance of 0.8 mm from the surface of UHMWPE and UHMWPE + 5 wt% of TPP by the number of carbon atoms (n) in the compound.

of UHMWPE. These species were identified in the flame from their mass spectrometric peaks with m/e 42, 54 and 78, whose intensities were the most intense of the 40 measured peaks. The concentrations of these species in the flame were measured using their calibration factors.

The profile of $[H_2O]$ was determined from the measured CO_2 concentration profile. The ratio $[H_2O]/[CO_2]$ was calculated for the maximum temperature by assuming thermodynamic equilibrium at this point during oxidation of the main pyrolysis products of propylene, butadiene, and benzene in air.

Using gas chromatography, concentration ratios were obtained for some species at a distance of ~ 0.8 mm, because this was not possible mass spectrometrically. In the sample taken, $[CO]$ and $[CO_2]$ were 3.2 and 9.7 vol%, respectively. In addition, the concentrations of the following species in vol% were found to be: H_2 : 0.68, CH_4 : 0.18, and C_2H_4 : 0.92. Oxygen was not found in the dripped melt and in the filtration residue. This indicates that thermal degradation on the burning surface proceeds without the participation of “diffuse” oxygen or that the formed oxidation products are highly volatile. When sampling the flame, the filters were coated with a white layer, presumably consisting of heavy hydrocarbons, formed during thermal degradation of polyethylene [8,9].

Figure 8a depicts the structure of a counterflow flame of UHMWPE without considering heavy degradation products; Fig. 8b gives the elemental mass balance, which shows the ratio $H/C \sim 1.2$ differs from its original value of 2 in UHMWPE. It is also to be noted that the mole fraction of CO_2 continuously grows as the distance from the burning surface diminishes, when it might have been expected to decrease. All this suggests that not all the combustion products have been considered in this system. These products are primarily heavy hydrocarbons formed during thermal degradation of UHMWPE and condensed on fine filters.

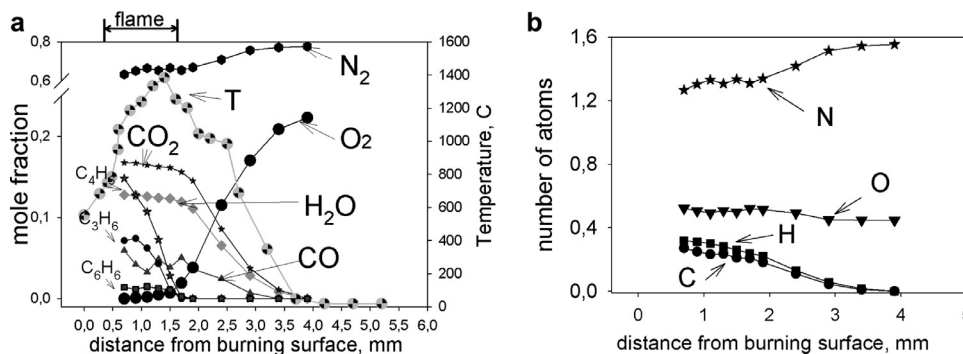


Fig. 8. The flame structure (a) and the elemental mass balance (b) in a UHMWPE flame.

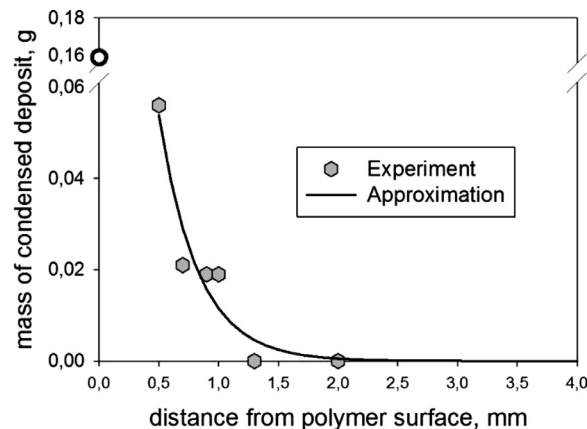


Fig. 9. Dependence of the mass of the pyrolysis products of UHMWPE condensed on the fine filters at the distance to the burning surface, L .

To consider the contribution of heavy hydrocarbons, the mass of condensed substances, deposited on the fine filters was measured. Figure 9 shows how the mass of condensed substances deposited on the filter varies with L , the distance to the burning surface, for a sampling time of 10 min. This dependence, measured with L between 0.5 and 2 mm, was approximated by an exponential relationship. The mass of condensed products right on the burning surface and indicated in Fig. 9 by the symbol \circ , was obtained by extrapolation.

3.4. The structure of a counterflow flame of UHMWPE considering heavy degradation products

Figure 10 shows the structure of a counterflow flame of UHMWPE as derived by considering the heavy hydrocarbons C_7 – C_{25} (indicated as “heavy” in Fig. 10) as only one hypothetical species with the average molecular weight of 258 g/mol. The concentration profiles of the light products of pyrolysing UHMWPE are shown in Fig. 10. The maximum temperature in the flame zone was 1380 °C. The profile of the mole fraction of heavy hydrocarbons was obtained by recalculating the dependence shown in Fig. 8 as follows. The mass of the condensed products was recalculated in moles by dividing it by the average molecular weight. The mole fraction of the gaseous products was calculated using the measured gas flux through the probe.

Since we added the profile of the mole fraction of the heavy products to the flame structure previously obtained (Fig. 8a), of course without considering them, we recalculated the mole fractions of every species. The sampling system did not allow $[H_2O]$ to be measured; therefore, it was calculated from the material balance equation arising from the ratio of the elements H and C in the

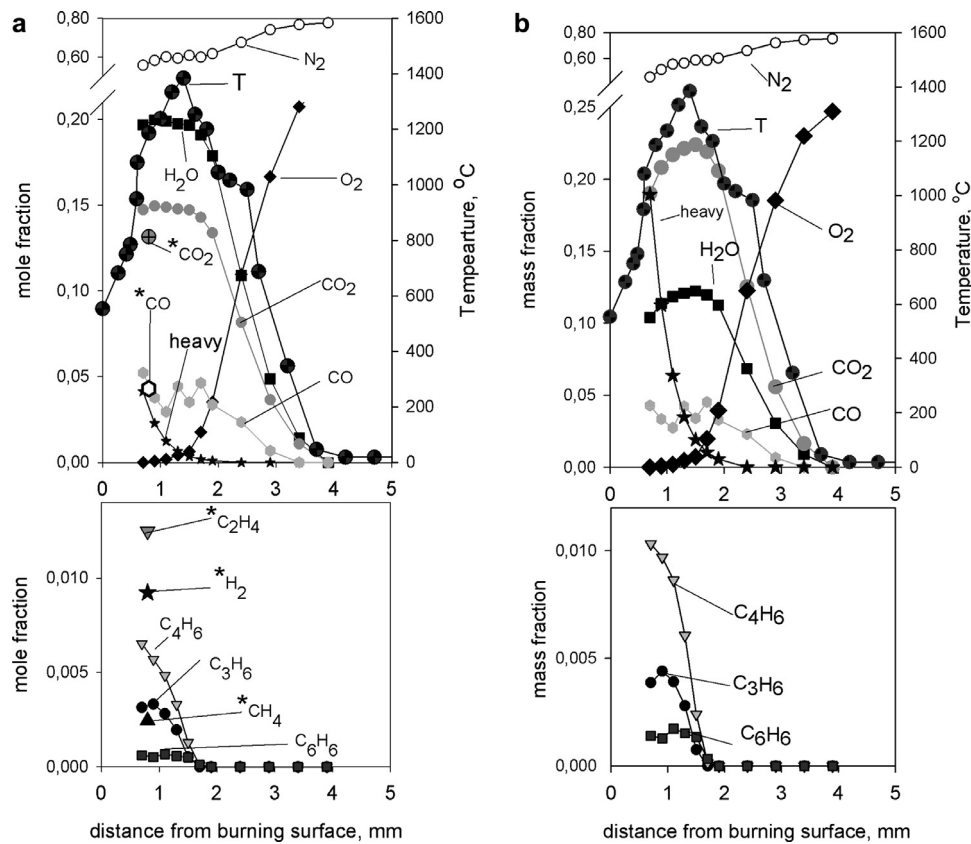


Fig. 10. The structure of counterflow flame of UHMWPE: (a) species' concentrations in mole fractions, (b) species' concentrations in mass fractions, (*) derived gas chromatographically when probe was at 0.8 mm from the burning surface.

Table 3

Mole fractions of the species and the flame temperature at a distance of 0.8 mm from the polyethylene's burning surface.

	T (°C)	N_2	O_2	CO_2	CO	H_2O	H_2	CH_4	C_2H_4	C_2H_6	C_3H_6	C_4H_6	C_6H_6	C_7-C_{25}
1	1180	0.58	0	0.14	0.04	0.2	0.009	0.002	0.012	–	0.003	0.006	0.0001	0.03
2	1270	0.72	0.002	0.11	0.05	0.14	0.001	0.004	^a 0.05	0.012	–	–	–	–
3	–	0.72	0.02	0.12	0.03	0.02	–	–	0.012	–	0.003	–	–	–

1– this study; 2 – [3]; 3 – [5].

^a – sum of C_2H_2 and C_2H_4 .

original polymer being 2. Figure 10a shows that, as the distance to the burning surface decreased, the mole fraction of condensed products increased. The zone of consumption of the combustible polymer degradation products was 1.7–1.8 mm. The concentration of O_2 at 1–1.2 mm from the burning surface dropped to zero. The accuracy of measuring $[O_2]$ was $\pm 0.3\%$. Assuming that heavy hydrocarbons did not affect any concentration profiles resulted in a significant reduction of the mass fraction of CO_2 and H_2O (Fig. 10b) near the burning surface. The mass fraction of heavy hydrocarbons (C_7-C_{25}) at a distance of 0.7 mm from the burning surface was ~ 0.2 . The existence of the large gradient of the concentrations of heavy hydrocarbons also allows an assumption to be made regarding their high concentration near the polymer.

The obtained estimate of the content of heavy hydrocarbons is a lower limit, as the experiments showed that, even with filters in the line delivering the sample to the mass spectrometer, a white deposit still appeared on the skimmer, although in much lower amounts than without filters.

Altogether, 10 species were identified in the pyrolysis products of the polymer, including water and the hypothetical substance with the molecular weight averaged over more than 50 hydrocarbons C_7-C_{25} .

Table 3 shows the concentration of the products and the temperature in the UHMWPE flame at a distance of 0.8 mm from its burning surface, obtained in this and a previous study [3,5]. The concentrations of H_2 , CH_4 , C_2H_4 were measured by gas chromatography; those of CO_2 , CO , H_2O , CH_4 , and C_2H_4 measured here are close to those measured before [3]. However, in previous measurements [3,5] only light hydrocarbons C_1-C_2 were identified. It can be seen from the profiles of the mole fractions shown above that $[CO_2]$ and $[CO]$ from gas chromatography are very close to those measured by mass spectrometry.

Increasing the molecular weight of polyethylene (UHMWPE) above that of the polyethylene studied in the literature, resulted in the appearance of new hydrocarbons, e.g. C_4H_6 and C_6H_6 in the pyrolysis products. Also C_3H_6 was identified; its concentration has been measured before [5]. In one study [3] only the sum $\{[C_2H_4] + [C_2H_2]\}$ was measured. The value of $[C_2H_4]$ measured previously [5] was close to that measured in this study.

The dependence of the ratio of the elements H/C in the combustion products from UHMWPE on the distance from the polymer is shown in Fig. 11, which demonstrates that the ratio $H/C \sim 2$, assuming that the products (in the entire combustion zone from

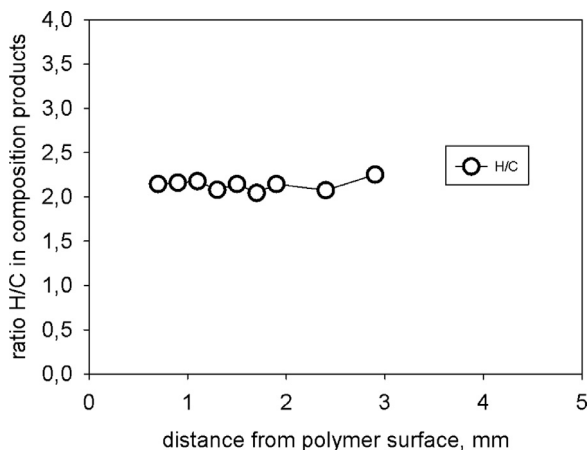


Fig. 11. Dependence of the ratio of H/C in the combustion products from UHMWPE on the distance from the polymer.

Table 4
Elemental analysis of the UHMWPE + 5 wt% of TPP.

	Original specimen (wt%)	Burning surface (wt%)	Dripped melt (wt%)
C	85.45	85.51	85.47
H	14.02	14.01	14.06
P	0.53	0.47	0.275

0.7 mm to 3 mm) from degrading the heavy polymer remain the same as that at ~2 mm.

3.5. The impact of TPP additive on the counterflow flame of UHMWPE

3.5.1. Analysis of the products condensed on a burning surface of UHMWPE +5 wt% TPP and of the products contained in the dripped melt

Important information was obtained on the processes in the condensed phase by analyzing the products formed on the polymer's burning surface, as well as of the products contained in the dripped melt, whilst burning UHMWPE +5 wt% of TPP. The techniques include elemental analysis, FTIR spectroscopy, and liquid chromatography/mass spectrometry (LC/MS). Table 4 demonstrates the results of the elemental analysis for burning UHMWPE +5 wt% of TPP. The original specimen, the extinguished burning surface, and the dripped melt formed by burning were all analyzed. The amount of phosphorus in the dripped melt was half that in the original specimen. Thus, half the original TPP remains in the condensed phase; the other half enters the gas phase.

The action of TPP in the condensed phase is also confirmed by analyzing the dripped melt formed during combustion of UHMWPE and UHMWPE + 5 wt% of TPP, using FTIR spectroscopy. Figure 12 shows the IR spectra of the dripped melt formed by burning UHMWPE and UHMWPE + 5 wt% of TPP. With TPP added to UHMWPE, lines emerged in the spectrum, corresponding to vibrations of the bonds P=O (1189 cm^{-1}) and P-O (966 cm^{-1}) in the IR spectrum of TPP. In the range of 1400–1000 cm^{-1} , a rich spectrum of phosphates, ethers, and carbonates emerged. This indicates that TPP interacts with the products from destroying UHMWPE in the condensed phase.

Interpretation of the IR spectrum of the melt from burning UHMWPE + 5 wt% of TPP is a difficult task. Therefore, in order to find out which products are formed in the condensed phase on the burning surface of the UHMWPE + 5 wt% of TPP, an extract of dripped melt obtained by soaking it in acetone

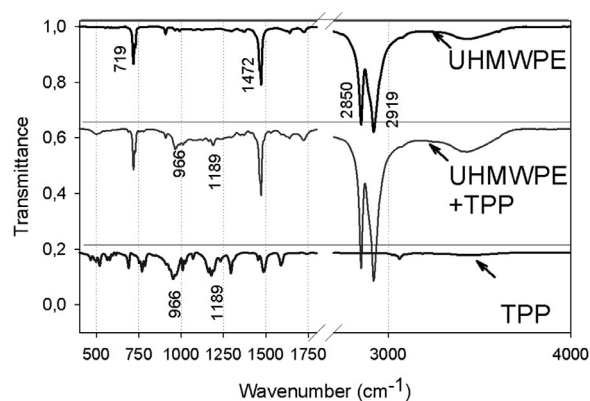


Fig. 12. IR spectra of TPP and of the dripped melt formed during combustion of UHMWPE and UHMWPE +5 wt% of TPP.

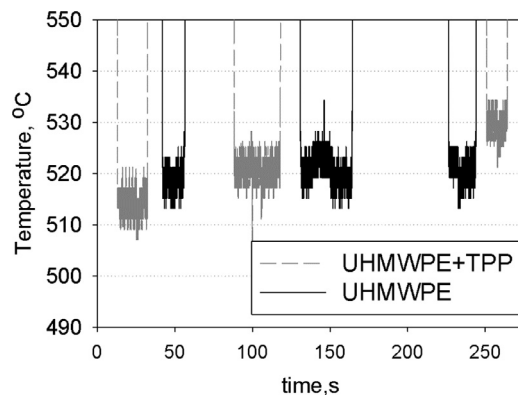


Fig. 13. Dependence of temperature on time in measuring the surface temperature: UHMWPE – solid line, UHMWPE +5 wt% of TPP – dashed line.

was analyzed. Its chromatographic analysis revealed such products as diphenyl-hydroxyphenyl-phosphate, 4-methyl-phenyl-diphenyl-phosphate, and 4-ethyl-phenyl-diphenyl-phosphate. A similar result was obtained previously [10].

3.5.2. The effect of TPP on the burning surface temperature and the temperature gradient in the condensed phase

The temperature of the UHMWPE burning surface in a counterflow flame was measured using two methods: (i) a thermocouple was moved through the flame until its junction touched the burning surface and (ii) a thermocouple was embedded in the specimen. The temperature corresponding to the moment the junction contacted the liquid was considered in the first case to be the surface temperature, when the thermocouple was enveloped with the molten layer. This moment was controlled visually. After that, the thermocouple's movement was stopped. The thermocouple remained motionless for several seconds, and then it was moved in the opposite direction. To raise the measurement's accuracy, the above procedure was repeated many times. Figure 13 shows how the measured temperature varies time when determining the surface temperature. As can be seen, the surface temperatures of UHMWPE without an additive and with 5 wt% of TPP added proved to be the same and equal to $522 \pm 8^\circ\text{C}$.

Whilst measuring the temperature with the thermocouple embedded in the specimen, the burning specimen was moved by a stepper motor without being rotated. The moment the thermocouple junction touched the burning surface was recorded with a Panasonic M3000 camera synchronized with the thermocouple's data acquisition module. Figure 14 shows slides from the video recording the moment when the thermocouple junction touched

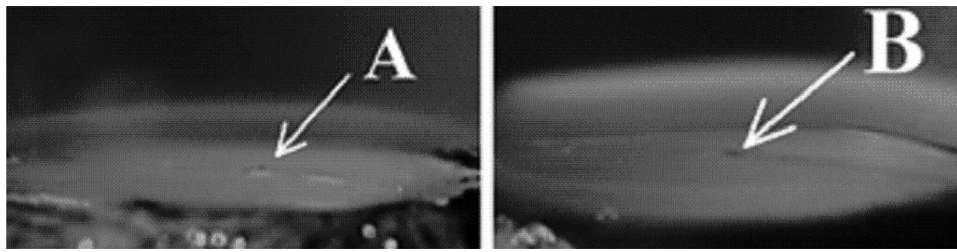


Fig. 14. Video slides of the thermocouple leaving the polymer: (A) UHMWPE and (B) UHMWPE + 5 wt% of TPP.

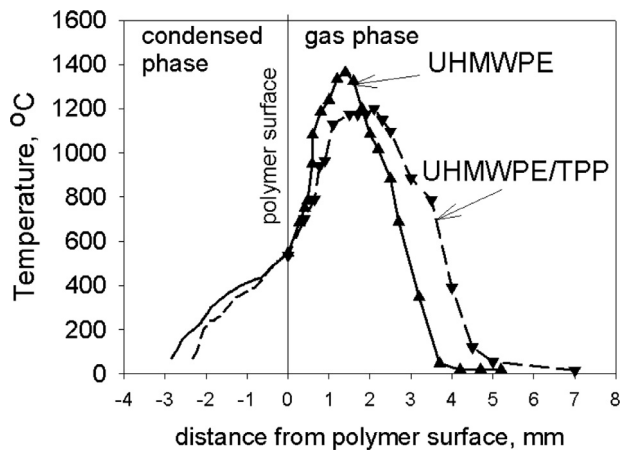


Fig. 15. The temperature profiles in the condensed and gas phases in burning UHMWPE: solid line – UHMWPE, dashed line – UHMWPE + 5 wt% of TPP.

the burning surface (an arrow indicates the thermocouple's junction), whereas Fig. 15 shows the temperature profiles in the condensed and gas phases obtained by both methods of measurement. The temperature gradient in the condensed phase near the burning surface was equal to 130 K/mm for UHMWPE and 100 K/mm for UHMWPE + 5 wt% of TPP. The temperature gradient in the gas phase near the burning surface was equal to 500 K/mm for UHMWPE and to 430 K/mm for UHMWPE + 5 wt% of TPP. The tem-

perature measured with the embedded molded-in thermocouple was 550 °C for UHMWPE and 530 °C for UHMWPE + 5 wt% of TPP. The temperature of the burning surface measured with an embedded thermocouple (550 °C) slightly exceeded that (522 °C) measured with the thermocouple moved in flame. However, within the limits of accuracy (± 15 °C) they are equal. One can also conclude that adding TPP to UHMWPE does not affect the temperature of the polymer's burning surface. The surface temperature of burning UHMWPE is close to that obtained previously [6]. The 14% reduction in the temperature gradient in the gas phase adjacent to the burning surface, when 5 wt% of TPP was added to UHMWPE indicates a corresponding reduction of the heat flux from the flame to the polymer when a flame retardant is present.

Adding 5 wt% of TPP changed the structure of the UHMWPE flame. In accordance with the temperature profile (Fig. 15), adding TPP to UHMWPE resulted in an increase of the total width of the flame zone by ~ 1.4 times (from 3.7 mm to 5 mm), a shift in the temperature maximum from 1.5 mm to 2.2 mm, and a decrease in the maximum temperature of 150 °C (from 1380 °C to 1230 °C).

3.5.3. The structure of a counterflow flame of UHMWPE+5 wt% of TPP

Figure 16 compares the flame structures of UHMWPE and UHMWPE + 5 wt% of TPP. Adding TPP resulted in the emergence of new mass peaks (m/e 50, 51, 65, 94) in the flame, typical of TPP. Due to the limited range of the measured masses in the Hiden HPR 60 mass spectrometer (1–300 m/e), it was not possible to find the parent TPP peak with a mass of 326 in the mass spectra of the

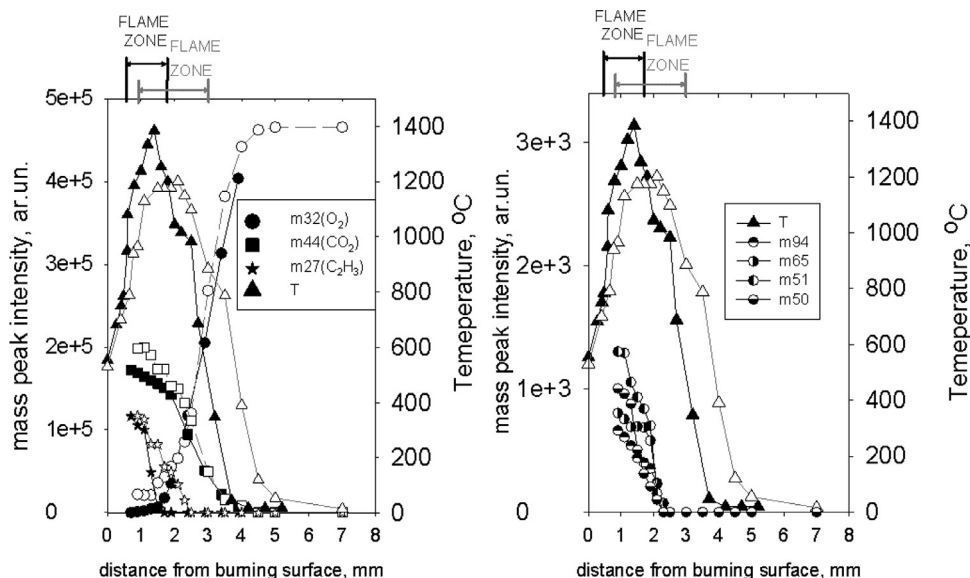


Fig. 16. Comparison of the temperature profiles and profiles of peak intensities for masses with m/e 27 ($C_2H_3^+$), 32 (O_2), 44 (CO_2) in flames of UHMWPE and UHMWPE + 5 wt% of TPP. Black symbols indicate data for a UHMWPE flame; colorless symbols are for a flame of UHMWPE+TPP.

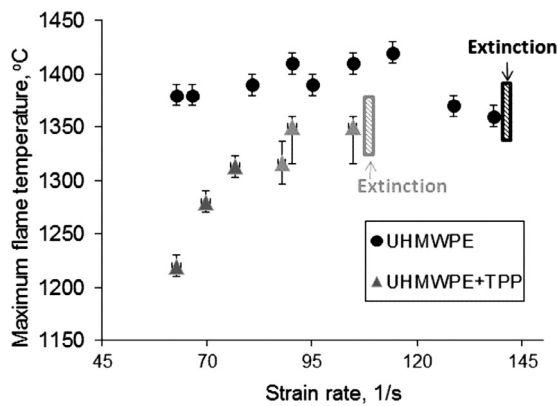


Fig. 17. Dependence of maximum flame temperature on the strain rate for UHMWPE and UHMWPE + 5 wt% of TPP.

samples taken from a counter-flow flame of UHMWPE+5 wt% of TPP. Such a peak has been identified previously [15] in the flame from burning UHMWPE +10% TPP during candle-like burning.

However, analysis of the peak intensities of masses with *m/e* 50, 51, 65, 94, in the mass spectrum of TPP and in the mass spectra of the samples from flames of UHMWPE and UHMWPE + 5 wt% of TPP allowed the presence of TPP to be established in the flame for UHMWPE + 5 wt% of TPP.

The consumption zone of the pyrolysis products was determined from the peak of the fragment ion ($C_2H_3^+$) with *m/e* of 27 and characteristic of most linear hydrocarbons. When 5 wt% of TPP was added to UHMWPE the pyrolysis zone shifted from 1.5 mm to 2.5 mm from the surface. This is close to the widened flame zone (from 1.3 mm to 2 mm) according to visual observations. In addition, a reduction of the hydrocarbons' oxidation rate in the reaction zone, when 5 wt% of TPP was added, resulted in the emergence of a small amount of O_2 at a distance of 0.7 mm from the burning surface. All these effects must be related to the flame-retarding impact of TPP on the gas phase oxidation reactions of the combustible products of thermal degradation of the polymer in the flame, because of the recombination of M and OM radicals in their reactions being catalysed phosphorus oxides [17].

3.6. The extinction limits of counterflow flames of UHMWPE and UHMWPE + 5 wt% of TPP

The extinction strain rate (ESR) is an important characteristic of a material's flammability determined by studying counter-flow flames. The strain rate (SR) *a* is determined for the combustion of gaseous and liquid fuels by the formula [22,23],

$$a = \frac{2V_{ox}}{L} \left(1 + \frac{V_{fuel}}{V_{ox}} \sqrt{\frac{\rho_{fuel}}{\rho_{ox}}} \right)$$

where V_{fuel} , V_{ox} , *L*, ρ_{fuel} , ρ_{ox} are the flow rate of the fuel and of the oxidizer, the distances between the nozzles and polymer's surfaces, and the densities of the fuel and oxidizers in the flows, respectively.

Figure 17 shows the dependence of the maximum flame temperature on the strain rate in counter-flow flames of UHMWPE and UHMWPE + 5 wt% of TPP. It can be noted that in the case of combustion of UHMWPE + 5 wt% of TPP, the maximum flame temperature grows on increasing the strain rate. However, beginning with the strain rate 90 s^{-1} , the flame of UHMWPE + 5 wt% of TPP becomes unstable. Therefore, intense oscillations begin in the area of the temperature maximum. Adding 5 wt% of TPP to UHMWPE leads to a reduction of the ESR by a factor of 1.4.

4. Discussion: the role of reactions in the condensed and gas phases during the flame retardancy of UHMWPE with TPP

Analysis of the data obtained indicates that reactions in the condensed and gas phases in the flame play different roles in the mechanism of flame retardancy of TPP for UHMWPE. Normally a conclusion regarding the effect of a flame retardant in the gas phase is based on the fact that it does not influence the thermal degradation of a polymer, determined by the TG and DTG methods, as was the case [11–13] when studying the action of TPP on the flammability of polycarbonate (PC) and PC/acrylonitrile-butadiene-styrene. However, it has been shown [15,16] that adding TPP to UHMWPE retards its thermal degradation in an inert atmosphere only at high heating rates ($\sim 150 \text{ K/s}$) and does not have any effect at low heating rates (0.17 K/s). This suggests that the above conclusion regarding the effect of a flame retardant in the gas phase is not always true. The following results obtained in this study show that the action of TPP in the condensed phase increases the flammability of UHMWPE:

1. The formation of phosphorus-containing compounds (phosphates, ethers, and carbonates) on a burning surface of UHMWPE+TPP reduces the share of TPP coming into the gas phase, where it effectively quenches radicals.
2. The reduction of the molecular weight of heavy hydrocarbon products from the thermal degradation of UHMWPE by about a factor of 2. Of course, lighter hydrocarbons burn at a higher burning rate.
3. The reduction of the polymer's burning rate results in a decrease in the flow rate of the degradation products from the burning surface of UHMWPE. This is expected to bring the flame zone closer to the burning surface and to increase the heat flux to it.
4. The increase of $[O_2]$ near the polymer's burning surface, found when TPP was added to the polymer, may only increase the heat release obtained previously [3] because of surface reactions oxidizing the polymer with oxygen diffusing from flame. The effect of small concentrations of O_2 (less than 1 vol%) diffusing to the burning surface on the kinetics and also the thermal effects of thermally degrading either UHMWPE or UHMWPE+TPP have not been previously investigated.

At the same time, the following facts established in this study confirm that there is a gas phase mechanism whereby TPP reduces a polymer's flammability.

1. Widening of the flame zone 1.5 times and a decrease of the maximum flame temperature by 150°C result in a reduction of the heat flux from the flame to the molten polymer. The latter was confirmed by direct measurements of the temperature gradients near the burning surface.
2. Reduction of the extinction strain rate by a factor of 1.4 is an important characteristic of a material's flammability. It was first detected in the system under study using a counter-flow diffusion flame of a polymer.
3. TPP is a well-known flame retardant for hydrocarbon flames.

Thus, although the presence of TPP in the condensed phase of a polymer results in a rise of its flammability, the effect of its action in the gas phase, resulting in the decrease of its flammability is more dominant. This leads to the fact that adding TPP to UHMWPE eventually reduces its flammability.

5. Summary and conclusion

This study continued previous investigations of the flammability of a model system consisting of a non-charring UHMWPE

polymer and organophosphorus flame retardant TPP, in which TPP was shown to be effective both in the condensed phase and in the flame with candle-like burning of UHMWPE. The counterflow flame method has been demonstrated to be applicable to studying the combustion of polymers with flame-retardant additives.

Using the counterflow flame method, as well as other diagnostic methods, such as on-line probing mass spectrometry, a microthermocouple technique, gas chromatography, GC, LC/MS, FTIR spectroscopy, and video recording, the burning rate of UHMWPE in a counterflow flame was measured. Also, the chemical and thermal flame structure were investigated, the burning surface temperature measured, together with the composition of the products of the polymer's destruction near the burning surface and the elemental composition of the species on the quenched burning surface. Furthermore, the effect of adding TPP to UHMWPE on these characteristics was investigated. Concentration profiles of 11 species (N_2 , O_2 , CO_2 , CO , H_2O , C_3H_6 , C_4H_6 , C_6H_6 , CH_4 , C_2H_4 , H_2) were measured and the concentration profile of a hypothetical species with a molecular weight of 258.7 g/mol averaged over more than 50 hydrocarbons C_7 – C_{25} . Elemental analysis showed half of the additive remained in the condensed phase, whereas the other half went into the gas phase. It was established that the action of TPP in the condensed phase increases UHMWPE's flammability; in the gas phase TPP reduces the flammability of UHMWPE. The effect of TPP's action in the gas phase is more dominant. This leads to the fact that adding TPP to UHMWPE eventually decreases its flammability. All the data obtained in this study of UHMWPE burning in a counterflow flame agree with earlier observations [15].

This study is the first step in obtaining qualitative data describing the combustion of polymers with and without a flame retardant, as well as for developing a model of the combustion of a polymer. Measurements of temperature profiles in the condensed phase and in the flame, of the temperature of the burning surface, of the burning rate, and of the flame's structure may be further used to develop a model of burning a polymer. The use of these techniques will provide data on the pyrolysis kinetics with and without a flame retardant added; application of molecular-beam mass spectrometry with soft ionization by electron impact will generate concentration profiles of both stable species and radicals in a flame. All this information is required for developing and validating any detailed mechanism of how a flame-retardant inhibits a flame, especially of a polymer.

Acknowledgments

The authors are thankful to Prof. V.A. Zakharov for the UHMWPE specimens provided and to Dr. M.M. Katasonov for providing assistance in anemometric measurements of the air flow rate profiles. This work was supported partially by the RFBF under Grants #16-58-53128 and #16-33-00230 and by the NNSF of China under Grant 51120165001.

References

- [1] H.F. Mark, N.M. Bikales, Ch.G. Overberger, G. Mendes, *Encyclopedia of polymer science and technology*, New York, 6, 1986, p. 490.

- [2] D.J. Holve, R.F. Sawyer, Diffusion controlled combustion of polymers, *Symp. (Int.) Combust.* 15 (1975) 351–361.
- [3] W.J. Pitz, N.J. Brown, R.F. Sawyer, The structure of a poly(ethylene) opposed flow diffusion flame, *Symp. (Int.) Combust.* 18 (1981) 1871–1879.
- [4] W.J. Pitz, N.J. Brown, and R.F. Sawyer, Flame structure measurement of polymer diffusion flames. Western States Section, The Combustion Institute, 1989, N°. 79–47.
- [5] J.R. Richard, C. Vovelle, R. Delbourgo, Flammability and combustion properties of polyolefinic materials, *Symp. (Int.) Combust.* 15 (1975) 205–216.
- [6] Y. Ogami, M. Mori, K. Yoshinaga, H. Kobayashi, Experimental study on polymer pyrolysis in high-temperature air diluted by H_2O and CO_2 using stagnation-point flow, *Combust. Sci. Technol.* 184 (2012) 735–749.
- [7] K. Seshadri, F.A. Williams, Structure and extinction of counterflow diffusion poly(methyl methacrylate) and its liquid monomer, both burning in nitrogen-air mixtures, *J. Polym. Sci.: Polym. Chem.* 16 (1978) 1755–1778.
- [8] J.A. Onwudili, N. Insura, P.T. Williams, Composition of products from the pyrolysis of polyethylene and polystyrene in a closed batch reactor: effects of temperature and residence time, *J. Anal. Appl. Pyrolysis* 86 (2009) 293–303.
- [9] N. Gascoin, G. Faua, P. Gillard, Experimental flash pyrolysis of high density polyethylene under hybrid propulsion conditions, *J. Anal. Appl. Pyrolysis* 101 (2013) 45–52.
- [10] B.N. Jang, C.A. Wilkie, The effects of triphenylphosphate and recorcinol-bis(diphenylphosphate) on the thermal degradation of polycarbonate in air, *Therm. Acta* 433 (2005) 1–12.
- [11] K.H. Pawlowski, B. Scharrel, Flame retardancy mechanisms of triphenyl phosphate, resorcinol bis(diphenyl phosphate) and bisphenol A bis(diphenyl phosphate) in polycarbonate/acrylonitrile-butadiene-styrene blends, *Polym. Int.* 56 (2007) 1404–1414.
- [12] B. Perret, K.H. Pawlowski, B. Scharrel, Fire retardancy mechanisms of arylphosphates in polycarbonate(PC) and PC/acrylonitrile-butadiene-styrene. The key role of decomposition temperature, *J. Therm. Anal. Calorim.* 97 (2009) 949–958.
- [13] B. Scharrel, Phosphorus-based flame retardancy mechanisms – old hat or a starting point for future development, *Materials* 3 (2010) 4710–4745.
- [14] M.W. Beach, N.G. Rondan, R.D. Froese, B.B. Gerhart, J.G. Green, B.G. Stobby, A.G. Shmakov, V.M. Shvartsberg, O.P. Korobeinichev, Studies of degradation enhancement of polystyrene by flame retardant additives, *Polym. Degrad. Stab.* 93 (2008) 1664–1673.
- [15] O.P. Korobeinichev, A.A. Paletsky, L.V. Kuibida, M.B. Gonchikzhpov, I.K. Shundrina, Reduction of flammability of ultrahigh-molecular-weight polyethylene by using triphenyl phosphate additives, *Proc. Combust. Inst.* 34 (2012) 2699–2706.
- [16] A.A. Paletsky, O.P. Korobeinichev, I.K. Shundrina, M.B. Gonchikzhpov, H. Chen, N. Liu, Influence of triphenyl phosphate on degradation kinetics of ultrahigh-molecular-weight polyethylene in inert and oxidative media, *Procedia Eng.* 62 (2013) 359–365.
- [17] O.P. Korobeinichev, V.M. Shvartsberg, A.G. Shmakov, The chemistry of combustion of organophosphorus compounds, *Russ. Chem. Rev.* 76 (2007) 1094–1121.
- [18] A.G. Shmakov, V.M. Shvartsberg, O.P. Korobeinichev, M.W. Beach, T.I. Hu, T.A. Morgan, Structure of a freely propagating rich CH_4 /air flame containing triphenylphosphine oxide and hexabromocyclododecane, *Combust. Flame* 149 (2007) 384–391.
- [19] M.W. Beach, T.A. Morgan, T.I. Hu, S.E. Vozar, S.Z. Filipi, V. Sick, A.G. Shmakov, V.M. Shvartsberg, O.P. Korobeinichev, Screening approaches for gas-phase activity of flame retardants, *Proc. Combust. Inst.* 32 (2009) 2625–2632.
- [20] A.G. Shmakov, V.M. Shvartsberg, O.P. Korobeinichev, M.W. Beach, T.I. Hu, T.A. Morgan, Effect of the addition of triphenylphosphine oxide, hexabromocyclododecane, and ethyl bromide on a $CH_4/O_2/N_2$ flame at atmospheric pressure, *Combust. Explos. Shock Waves* 43 (2007) 501–508.
- [21] A. Ishihara, Y. Sakai, K. Konishi, E. Andoh, Correlation between burning surface temperature and regression rate for polymethylmethacrylate, *Proc. Combust. Inst.* 30 (2005) 2123–2130.
- [22] K. Seshadri, F.A. Williams, Laminar flow between parallel plates with injection of a reactant at high Reynolds number, *Int. J. Heat Mass Transfer* 21 (1978) 251–253.
- [23] M.A. Macdonald, T.M. Jayaweera, E.M. Fisher, F.C. Gouldin, variation of chemically active and inert flame-suppression effectiveness with stoichiometric mixture fraction, *Symp. (Int.) Combust.* 27 (1998) 2749–2766.